MoBi implementation of the Dancik et al. skin permeation model

Abdullah Hamadeh, Michael Sevestre, Andrea Edginton

1   Introduction

This document is a user guide to a MoBi implementation of the skin permeation model in (Dancik et al. 2013). In that model, the skin is a multilayered slab into which an applied permeant diffuses. Each of the slab layers in the model corresponds to an anatomical skin layer and inherits its diffusion parameters from the physical and chemical properties of the layer. In MoBi, the user enters parameters describing the skin, ambient conditions, experimental conditions, the permeant, the vehicle (if any) and dosage conditions. Simulation of the model returns:

- amounts of permeant present at different skin depths, over the time of the simulation,
- the amount of permeant that has escaped the vehicle and skin through evaporation,
- the cumulative amount and the flux, over time, of permeant that has crossed the entire skin membrane (for *in vitro* simulations) or cleared the dermis into the bloodstream (for *in vivo* simulations).

This document is organized as follows: the theoretical skin model implemented in MoBi is presented next, followed by a guide to the user interface.

1.1   What this package contains

File name	Description
skin_permeation_model.mbp3	Main MoBi project file containing the skin permeation model. This file was made using MoBi 7.4.
skin_spatial_structure.pkml	PKML file containing the spatial structure of the PKML model.
skin_template.mbdt	File containing the graphical layout of the skin model spatial structure.
OSPSuite.Dimensions	File containing dimension definitions specific to the skin permeation model. For Windows users this file should typically reside in the directoty C:\ProgramData\Open Systems Pharmacology\MoBi\X.X, with X.X representing the MoBi release number.
skin_favorites.xml	File to load list of input parameters for simulating the skin model.

2   Theoretical model

The model assumes the skin structure shown in Figure 1. The skin slab is of cross-sectional area A and consists of three stacked layers: the stratum corneum (SC), the viable epidermis (ED) and the dermis (DE). The permeant is applied on top of the SC layer, and diffuses downwards into the layers below.
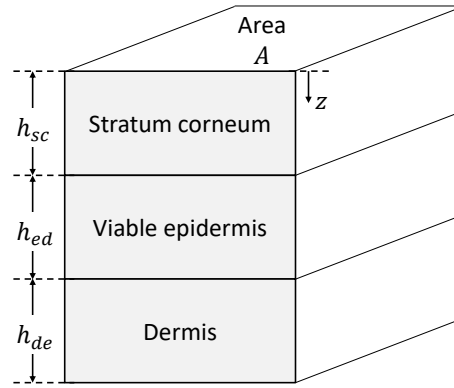
Figure 1: Structure of skin slab used in model.

Diffusion into the skin, along the z direction, is modeled using a one-dimensional diffusion equation in the SC and ED layers. Permeation in the DE layer is also modeled as a one-dimensional diffusion equation, but, for *in vivo* simulations, this layer includes an added clearance term that models permeant clearance into the bloodstream. An additional metabolism term, not modeled in (Dancik et al. 2013), is also optionally available in both the ED and DE layers. The concentrations in the three layers are denoted respectively as $c_{sc}(z,t)$ for $0 \leq z < h_{sc}$, $c_{ed}(z,t)$ for $h_{sc} \leq z < h_{sc} + h_{ed}$, and $c_{de}(z,t)$ for $h_{sc} + h_{ed} \leq z \leq h_{sc} + h_{ed} + h_{de}$.

Nomenclature	
K_{sc}	Partition coefficient of permeant in stratum corneum relative to water.
D_{sc}	Stratum corneum diffusion constant.
K_{ed}	Partition coefficient of permeant in viable epidermis relative to water.
D_{ed}	Viable epidermis diffusion constant.
K_{de}	Partition coefficient of permeant in dermis relative to water.
D_{de}	Dermis diffusion constant.
k_{de}	Dermis clearance rate constant.
ρ	Density of permeant.
k_{evap}	Rate of evaporation of permeant.
V_{max}	Michaelis-Menten saturation rate of metabolic degradation of permeant.
K_M	Permeant concentration at half-saturation rate of metabolic degradation.

Two boundary conditions hold at the SC/ED interface and the ED/DE interface: first, mass continuity requires that the flux leaving one layer enters the next. From Fick's law, this implies that the partial derivatives of permeant concentration with respect to z on the two sides of the interface are related by the ratio of the diffusion coefficients on the two sides. Second, the permeant concentrations at the two sides of the interface are related by the ratios of permeant's partition coefficient in the two layers.

In the case of in vivo simulations, it is assumed that there is no flux out of the dermis except though clearance into the bloodstream. A no-flux boundary condition therefore holds at the bottom of the dermis in the *in vivo* case. For in vitro simulations, it is assumed that the bottom layer of the dermis is in direct

contact with a zero-concentration receptor solution into which the permeant diffuses. For this reason, the boundary condition at the base of the dermis maintains the concentration there at zero in *in vitro* simulations.

The diffusion of the permeant into the skin are modeled in two distinct scenarios that each impose different boundary conditions at the vehicle/SC interface:

   i.   the permeant is applied in a volatile vehicle or neat,
   ii. the permeant is applied in an immobile vehicle.

Each scenario will be discussed in turn.

2.1   Neat/volatile vehicle case

It is assumed that prior to application of the dose, the skin slab is free of the permeant. Upon application of a dose of mass M_0, the permeant is distributed uniformly in the deposition zone, which is the top segment of the SC layer, and the thickness of which (h_{dep}) depends on the type of vehicle used. The deposition zone is saturated when the mass concentration of permeant reaches a value C_{sat}.

If the dose has a mass M_{surf} in excess of the permeant mass that saturates the deposition zone (a scenario denoted Case 2 in (Dancik et al. 2013)), the initial conditions are such that the concentration in the deposition zone is C_{sat} and the excess dose lies in a pool atop the SC. Following (Kasting and Miller 2006), while the pool remains un-depleted, the flow of permeant from the pool and into the deposition zone is assumed to remain equal to the flow of the permeant out of the bottom of the deposition zone and into the rest of the SC. In this way the concentration of permeant in the deposition zone remains constant at C_{sat} until the pool is depleted. Simultaneously, the permeant may evaporate from the excess pool at a rate $k_{evap} \cdot \rho$, where ρ is the density of the permeant and k_{evap} is derived in (Dancik et al. 2013; Kasting and Miller 2006). The region of the SC below the deposition zone is assumed to follow a one-dimensional diffusion equation with diffusion coefficient D_{sc}. Cases 1 and 2 are illustrated in Figure 2.

Upon depletion of this pool, the simulation reverts to a scenario denoted Case 1 in (Dancik et al. 2013). Here, diffusion in the entire SC is governed by a one-dimensional diffusion equation with diffusion coefficient D_{sc}. Evaporation from the top of the SC layer occurs at a rate $k_{evap} \cdot \rho \cdot c_{sc}(0,t)/C_{sat}$.

In both cases 1 and 2, diffusion in the ED region obeys a one-dimensional diffusion-decay equation with diffusion coefficient D_{ed} and decay rate given by a Michaelis-Menten term $f_m(c_{ed})$ (see equation (1) below) representing metabolism. Diffusion in the DE region also obeys a one-dimensional diffusion-decay equation with diffusion coefficient D_{de}, an *in vivo*–only clearance term k_{de} and a metabolic decay term $f_m(c_{de})$. The mathematical models describing Cases 1 and 2 are given in Table 1. In Table 1, the dermis clearance rate constant is given by $k_{de} = \frac{k_{free}}{BindingFactor}$ where $k_{free} = \frac{1}{\frac{1}{P_{cap} \cdot S} + \frac{1}{Q}}$ is the dermis clearance rate constant of molecules in the dermis that are not bound to protein and where the factor $BindingFactor$ corrects for protein binding. In the definition of k_{free}, P_{cap}, measured in cm.h⁻¹, is, from and (Potts and Guy 1992), given by

$$\log P_{cap} = -2.74 + \left(0.71 \log K_{o/w}\right) - 0.0061 \cdot MW + \log m$$

S is the capillary surface area per unit volume and Q is the blood-flow limited capillary clearance, as defined in (Dancik et al. 2013) and, from (Fedorowicz et al. 2011), $m = 100$. The rate of metabolism in the viable epidermis and dermis is given by

$$f_m(c) = V_{max} \frac{c}{c + K_M} \tag{1}$$

2.2   Immobile vehicle case

As with the volatile vehicle case, it is assumed that prior to application of the dose, the skin slab is free of the permeant. Upon application of a dose of mass M_0, the permeant is distributed between the deposition zone of the SC, a vehicle layer above the SC and, if the dose is large, a pool of permeant above the vehicle layer. The deposition zone and the vehicle layer are both saturable at mass concentrations C_{sat} and S_v respectively (see (Dancik et al. 2013) for derivations). The mass of the permeant in the surface pool, M_{surf}, is the mass of the permeant amount in excess of that which saturates the deposition zone and the vehicle. If such a saturating dose is applied, the simulation starts under the conditions of Case 4 in (Dancik et al. 2013). If the applied dose is not sufficient to saturate both the deposition zone and the vehicle (Case 3 in (Dancik et al. 2013)), the permeant is initially distributed between the two layers such that the two layers have the same saturation fraction. Cases 3 and 4 are illustrated in Figure 3.

While the pool remains un-depleted, the flux of permeant from the pool and into the vehicle layer equals the flux from the vehicle layer and into the deposition zone and also equals the flux from the deposition zone into the lower layers of the SC. In this way, the concentrations of permeant in the vehicle layer and the deposition zone remain constant at S_v and C_{sat} until the surface pool is depleted. Simultaneously, the permeant may evaporate from the pool at a rate $k_{evap} \cdot \rho$, where ρ is the density of the permeant and k_{evap} is derived in (Dancik et al. 2013; Kasting and Miller 2006). The region of the SC below the deposition zone is assumed to follow a one-dimensional diffusion equation with diffusion coefficient D_{sc}.

Upon depletion of this pool, the simulation reverts to Case 3. Note that at this time point both the vehicle and deposition zone are at full saturation. Diffusion in the entire SC is, henceforth, governed by a one-dimensional diffusion equation with diffusion coefficient D_{sc}. Evaporation from the vehicle layer occurs at a rate $k_{evap} \cdot \rho \cdot c_v(t)/S_v$.

In both cases 3 and 4, diffusion in the ED region obeys a one-dimensional diffusion-decay equation with diffusion coefficient D_{ed} and decay rate given by a Michael-Menten term f_m representing metabolism. Diffusion in the DE region also obeys a one-dimensional diffusion-decay equation with diffusion coefficient D_{de} and decay terms due to in vivo clearance (with rate constant k_{de}) and due to metabolism (with rate f_m). The mathematical models describing Cases 3 and 4 are given in Table 2. The terms k_{de} and f_m are defined as in Cases 1 and 2.

Case 1

Initial conditions

$$c_{sc}(z,0) = \frac{M_0}{h_{dep} \cdot A}, 0 \le z < h_{dep}$$

$$c_{sc}(z,0) = 0, h_{dep} \le z < h_{sc}$$

$$c_{ed}(z,0) = 0, h_{sc} \le z < h_{sc} + h_{ed}$$

$$c_{de}(z,0) = 0, h_{sc} + h_{ed} \le z < h_{sc} + h_{ed} + h_{de}$$

Boundary conditions

$$D_{sc} \frac{\partial c_{sc}(0,t)}{\partial z} = k_{evap} \cdot \rho \cdot c_{sc}(0,t)/C_{sat}$$

$$\frac{c_{sc}(h_{sc},t)}{K_{sc}} = \frac{c_{ed}(h_{sc},t)}{K_{ed}}$$

$$D_{sc} \frac{\partial c_{sc}(h_{sc},t)}{\partial z} = D_{ed} \frac{\partial c_{ed}(h_{sc},t)}{\partial z}$$

$$\frac{c_{ed}(h_{sc}+h_{ed},t)}{K_{ed}} = \frac{c_{de}(h_{sc}+h_{ed},t)}{K_{de}}$$

$$D_{ed} \frac{\partial c_{ed}(h_{sc}+h_{ed},t)}{\partial z} = D_{de} \frac{\partial c_{de}(h_{sc}+h_{ed},t)}{\partial z}$$

$$\frac{\partial c_{de}(h_{sc}+h_{ed}+h_{de},t)}{\partial z} = 0 \quad \text{(in vivo case)}$$

$$c_{de}(h_{sc}+h_{ed}+h_{de},t) = 0 \quad \text{(in vitro case)}$$

Dynamics

$$\frac{\partial c_{sc}(z,t)}{\partial t} = \frac{\partial^2 c_{sc}(z,t)}{\partial z^2}, \text{for } 0 \le z < h_{sc}$$

$$\frac{\partial c_{ed}(z,t)}{\partial t} = \frac{\partial^2 c_{ed}(z,t)}{\partial z^2} - f_m(c_{ed}), \text{for } h_{sc} \le z < h_{sc} + h_{ed}$$

$$\frac{\partial c_{de}(z,t)}{\partial t} = \frac{\partial^2 c_{de}(z,t)}{\partial z^2} - k_{de}c_{de}(z,t) - f_m(c_{de}),$$

for $h_{sc} + h_{ed} \le z < h_{sc} + h_{ed} + h_{de}$

$k_{de} > 0$ (in vivo case)

$k_{de} = 0$ (in vitro case)

Case 2

$$c_{sc}(z,0) = C_{sat}, 0 \le z < h_{dep}$$

$$c_{sc}(z,0) = 0, h_{dep} \le z < h_{sc}$$

$$c_{ed}(z,0) = 0, h_{sc} \le z < h_{sc} + h_{ed}$$

$$c_{de}(z,0) = 0, h_{sc} + h_{ed} \le z < h_{sc} + h_{ed} + h_{de}$$

$$\frac{dM_{surf}(t)}{dt} = -D_{sc} \frac{\partial c_{sc}(h_{dep},t)}{\partial z} - k_{evap} \cdot \rho$$

$$\frac{c_{sc}(h_{sc},t)}{K_{sc}} = \frac{c_{ed}(h_{sc},t)}{K_{ed}}$$

$$D_{sc} \frac{\partial c_{sc}(h_{sc},t)}{\partial z} = D_{ed} \frac{\partial c_{ed}(h_{sc},t)}{\partial z}$$

$$\frac{c_{ed}(h_{sc}+h_{ed},t)}{K_{ed}} = \frac{c_{de}(h_{sc}+h_{ed},t)}{K_{de}}$$

$$D_{ed} \frac{\partial c_{ed}(h_{sc}+h_{ed},t)}{\partial z} = D_{de} \frac{\partial c_{de}(h_{sc}+h_{ed},t)}{\partial z}$$

$$\frac{\partial c_{de}(h_{sc}+h_{ed}+h_{de},t)}{\partial z} = 0 \quad \text{(in vivo case)}$$

$$c_{de}(h_{sc}+h_{ed}+h_{de},t) = 0 \quad \text{(in vitro case)}$$

$$c_{sc}(z,t) = C_{sat}, \text{for } 0 \le z < h_{dep}$$

$$\frac{\partial c_{sc}(z,t)}{\partial t} = \frac{\partial^2 c_{sc}(z,t)}{\partial z^2}, \text{for } h_{dep} \le z < h_{sc}$$

$$\frac{\partial c_{ed}(z,t)}{\partial t} = \frac{\partial^2 c_{ed}(z,t)}{\partial z^2} - f_m(c_{ed}), \text{for } h_{sc} \le z < h_{sc} + h_{ed}$$

$$\frac{\partial c_{de}(z,t)}{\partial t} = \frac{\partial^2 c_{de}(z,t)}{\partial z^2} - k_{de}c_{de}(z,t) - f_m(c_{de}),$$
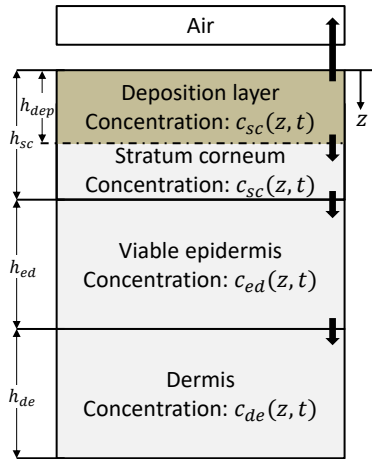
for $h_{sc} + h_{ed} \le z < h_{sc} + h_{ed} + h_{de}$

$k_{de} > 0$ (in vivo case)

$k_{de} = 0$ (in vitro case)

Table 1: Theoretical descriptions of Cases 1 and 2.
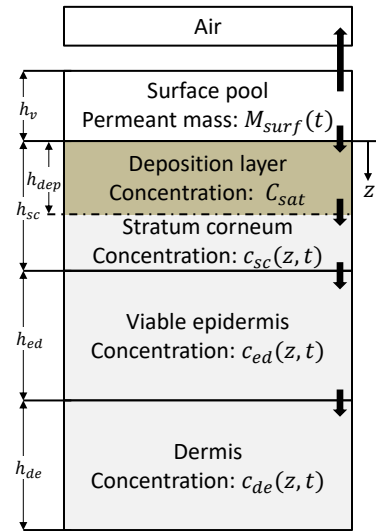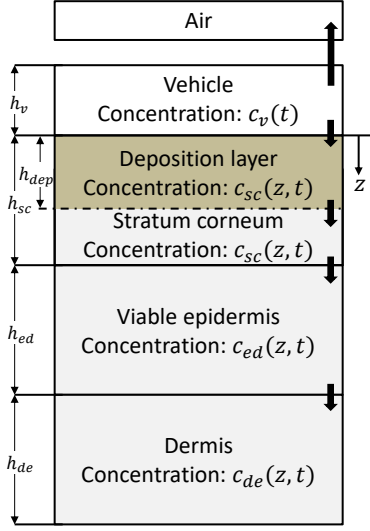
Case 1

Case 2

Figure 2: Diffusion in cases where the permeant is applied neat or in a volatile vehicle.
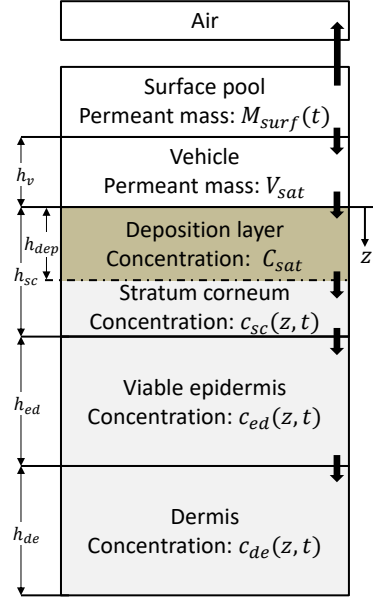
Case 3

Case 4

Figure 3: Diffusion in cases where the permeant is applied via an immobile vehicle.

Case 3	Case 4
Initial conditions	

Case 3

Initial conditions

$$c_v(0) = M_0 \frac{S_v}{S_v \cdot h_v \cdot A + C_{sat} \cdot h_{dep} \cdot A}$$

$$c_{sc}(z,0) = M_0 \frac{C_{sat}}{S_v \cdot h_v \cdot A + C_{sat} \cdot h_{dep} \cdot A}, \text{ for } 0 \leq z < h_{dep}$$

$$c_{sc}(z,0) = 0, \text{ for } h_{dep} \leq z < h_{sc}$$

$$c_{ed}(z,0) = 0, \text{ for } h_{sc} \leq z < h_{sc} + h_{ed}$$

$$c_{de}(z,0) = 0, h_{sc} + h_{ed} \leq z < h_{sc} + h_{ed} + h_{de}$$

Boundary conditions

$$\frac{dc_v(t)}{dt} = -k_{evap} \cdot \rho \cdot \frac{c_v(t)}{S_v} - D_{sc} \frac{\partial c_{sc}(0,t)}{\partial z}$$

$$\frac{c_{sc}(h_{sc},t)}{K_{sc}} = \frac{c_{ed}(h_{sc},t)}{K_{ed}}$$

$$D_{sc} \frac{\partial c_{sc}(h_{sc},t)}{\partial z} = D_{ed} \frac{\partial c_{ed}(h_{sc},t)}{\partial z}$$

$$\frac{c_{ed}(h_{sc}+h_{ed},t)}{K_{sc}} = \frac{c_{de}(h_{sc}+h_{ed},t)}{K_{ed}}$$

$$D_{ed} \frac{\partial c_{ed}(h_{sc}+h_{ed},t)}{\partial z} = D_{de} \frac{\partial c_{de}(h_{sc}+h_{ed},t)}{\partial z}$$

$$\frac{\partial c_{de}(h_{sc} + h_{ed} + h_{de}, t)}{\partial z} = 0 \quad \text{(in vivo case)}$$

$$c_{de}(h_{sc} + h_{ed} + h_{de}, t) = 0 \quad \text{(in vitro case)}$$

Dynamics

$$\frac{\partial c_{sc}(z,t)}{\partial t} = \frac{\partial^2 c_{sc}(z,t)}{\partial z^2}, \text{ for } 0 \leq z < h_{sc}$$

$$\frac{\partial c_{ed}(z,t)}{\partial t} = \frac{\partial^2 c_{ed}(z,t)}{\partial z^2} - f_m\big(c_{ed}(z,t)\big), \text{ for } h_{sc} \leq z < h_{sc} + h_{ed}$$

$$\frac{\partial c_{de}(z,t)}{\partial t} = \frac{\partial^2 c_{de}(z,t)}{\partial z^2} - k_{de}c_{de}(z,t) - f_m\big(c_{de}(z,t)\big),$$
$$\text{for } h_{sc} + h_{ed} \leq z < h_{sc} + h_{ed} + h_{de}$$
$$k_{de} > 0 \quad \text{(in vivo case)}$$
$$k_{de} = 0 \quad \text{(in vitro case)}$$

Case 4

Initial conditions

$$c_v(0) = S_v$$

$$c_{sc}(z,0) = C_{sat}, \text{ for } 0 \leq z < h_{dep}$$

$$c_{sc}(z,0) = 0, \text{ for } h_{dep} \leq z < h_{sc}$$

$$c_{ed}(z,0) = 0, \text{ for } h_{sc} \leq z < h_{sc} + h_{ed}$$

$$c_{de}(z,0) = 0, \text{ for } h_{sc} + h_{ed} \leq z < h_{sc} + h_{ed} + h_{de}$$

Boundary conditions

$$\frac{dM_{surf}}{dt} = -k_{evap} \cdot \rho - D_{sc} \frac{\partial c_{sc}(h_{dep},t)}{\partial z}$$

$$\frac{c_{sc}(h_{sc},t)}{K_{sc}} = \frac{c_{ed}(h_{sc},t)}{K_{ed}}$$

$$D_{sc} \frac{\partial c_{sc}(h_{sc},t)}{\partial z} = D_{ed} \frac{\partial c_{ed}(h_{sc},t)}{\partial z}$$

$$\frac{c_{ed}(h_{sc}+h_{ed},t)}{K_{sc}} = \frac{c_{de}(h_{sc}+h_{ed},t)}{K_{ed}}$$

$$D_{ed} \frac{\partial c_{ed}(h_{sc}+h_{ed},t)}{\partial z} = D_{de} \frac{\partial c_{de}(h_{sc}+h_{ed},t)}{\partial z}$$

$$\frac{\partial c_{de}(h_{sc} + h_{ed} + h_{de}, t)}{\partial z} = 0 \quad \text{(in vivo case)}$$

$$c_{de}(h_{sc} + h_{ed} + h_{de}, t) = 0 \quad \text{(in vitro case)}$$

Dynamics

$$c_{sc}(z,t) = C_{sat}, \text{ for } 0 \leq z < h_{dep}$$

$$\frac{\partial c_{sc}(z,t)}{\partial t} = \frac{\partial^2 c_{sc}(z,t)}{\partial z^2}, \text{ for } h_{dep} \leq z < h_{sc}$$

$$\frac{\partial c_{ed}(z,t)}{\partial t} = \frac{\partial^2 c_{ed}(z,t)}{\partial z^2} - f_m\big(c_{ed}(z,t)\big), \text{ for } h_{sc} \leq z < h_{sc} + h_{ed}$$

$$\frac{\partial c_{de}(z,t)}{\partial t} = \frac{\partial^2 c_{de}(z,t)}{\partial z^2} - k_{de}c_{de}(z,t) - f_m\big(c_{de}(z,t)\big),$$
$$\text{for } h_{sc} + h_{ed} \leq z < h_{sc} + h_{ed} + h_{de}$$
$$k_{de} > 0 \quad \text{(in vivo case)}$$
$$k_{de} = 0 \quad \text{(in vitro case)}$$

Table 2: Theoretical descriptions of Cases 3 and 4.

2.3 Deviations of MoBi model from Dancik et al., 2013

In addition to the inclusion of the metabolism terms f_m in the viable tissue, the model implemented in MoBi differs from the published model in (Dancik et al. 2013) in several respects:

- In Cases 2 and 4, the boundary conditions at the top SC boundary are modified from B.17 and B.19 in (Dancik et al. 2013) to include the flux from the surface pool into the SC. In addition, evaporation from the surface pool is modified to the form given in equation 7 in (Kasting and Miller 2006). Note that the M_{surf} is differentiated with respect to time, and not distance z, as in equations B.17 and B.19 in (Dancik et al. 2013).
- In Case 3, the boundary condition at the top SC boundary is modified to be a function of the derivative of the vehicle permeant concentration with respect to time, and not distance z, as in equation B.18.
- Following (Fedorowicz et al. 2011), the permeant's SC/water partition coefficient is not modified as in equation in C.12 in (Dancik et al. 2013).

3 Implementation of model in MoBi

The MoBi implementation of the model described in the preceding structure is contained in the file **skin_permeation_model.mbp3**. It has an air compartment **air**, a surface pool compartment **surface_pool**, a vehicle compartment **vehicle**, a skin compartment **skin_compartment** and two sink compartments, **in_vivo_sink** and **in_vitro_sink** (Figure 4, left). The compartment **skin_compartment** is made up of three compartments that represent the different skin sublayers: a stratum corneum compartment **SC_skin_sublayer**, a viable epidermis compartment **ED_skin_sublayer**, and a dermis compartment **DE_skin_sublayer** (Figure 4, right). Each of these three skin sublayer compartments consists of four sub-compartments (labelled **comp10_1** to **comp10_4**, as in Figure 5, left), each of which is composed of ten sub-sub-sublayers (labelled **layer1** to **layer10**, as in Figure 5). Therefore, as per the model in (Dancik et al. 2013), each of **SC_skin_sublayer**, **ED_skin_sublayer**, and **DE_skin_sublayer** are composed of forty skin sub-sub-layers in total. The sub-sublayers each represent a slice of skin at a specific skin depth. The model simulates the permeant in the **vehicle** compartment as entering **skin_compartment** at **layer1** of **comp10_1** of **SC_skin_sublayer**. Dermal clearance of the permeant can occur in one of two ways:

- in *in vivo* simulations, the permeant undergoes passive transport from all layers of the **DE_skin_sublayer** into bloodstream, represented by the **in_vivo_sink** compartment, or,
- in *in vitro* simulations, the permeant diffuses out of **layer10** of **comp10_4** of **DE_skin_sublayer** and into the **in_vitro_sink** compartment, which represents a receptor solution of zero permeant concentration.

The diffusion of permeant from one sub-sub-layer to another is numerically computed using the method of finite differences and Fick's law, which models the one-dimensional diffusive flux J (amount per unit area per unit time) at spatial position z, at time t, in the direction of increasing z as $J(z,t) = -D\frac{\partial c(z,t)}{\partial z}$, where D is the medium's diffusion coefficient and $c(z,t)$ is the concentration of the permeant at position z.

As an illustrative example, Figure 6 shows three sub-sub-layers of the viable epidermis. The individual layers are assumed to be thin enough that the concentration within each is approximately constant.

Viewed from the top, these skin layers would have a cross-sectional area A, as in Figure 1 (not shown in Figure 6). The rate of flow of permeant from layer $i - 1$ to layer i is, from Fick's law, approximately given by the quantity $D_{ED} \cdot \frac{c_{ED_{i-1}} - c_{ED_i}}{\delta_{ED}} \cdot A$. Similarly, the flow from layer i to $i + 1$ is given by $D_{ED} \cdot \frac{c_{ED_i} - c_{ED_{i+1}}}{\delta_{ED}} \cdot A$. At the same time, the model allows for metabolic reactions that consume the permeant. In layer i, this takes place at rate $f_m(c_{ED_i})$. Therefore the net rate of change of the concentration of permeant in layer i is approximated by

$$\frac{\partial c_{ED_i}}{\partial t} \approx \frac{1}{\delta_{ED}} \left(D_{ED} \cdot \frac{c_{ED_{i-1}} - c_{ED_i}}{\delta_{ED}} - D_{ED} \cdot \frac{c_{ED_i} - c_{ED_{i+1}}}{\delta_{ED}} \right) - f_m(c_{ED_i})$$

which equals the finite difference approximates approximation of the diffusion-decay equations for the viable epidermis in Table 1 and Table 2.
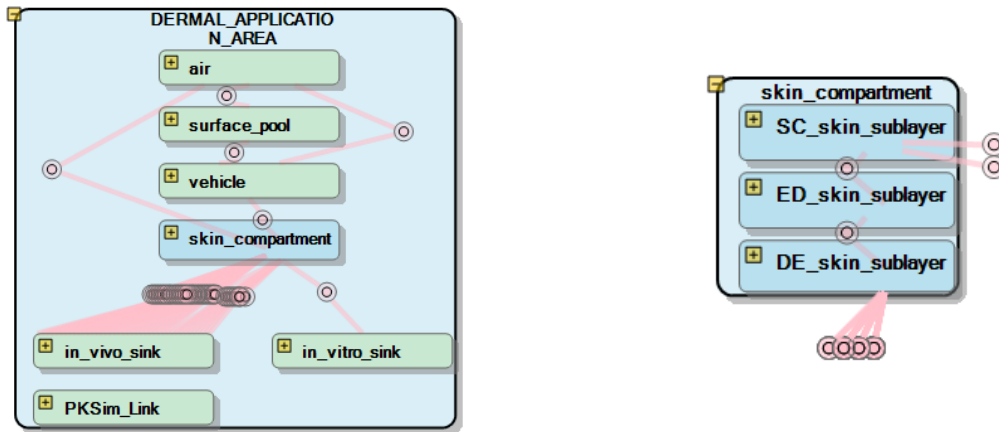

Figure 4: Left, overview of entire skin permeation model, right, sub-compartments of skin compartment. Pink connector lines represent possible permeant transport pathways.

Figure 5: Skin sublayers are each divided into four sub-compartments, as shown for the viable epidermis sublayer in the left figure. Each compartment is divided into ten further sub-compartments (right). Pink connector lines represent possible permeant transport pathways.
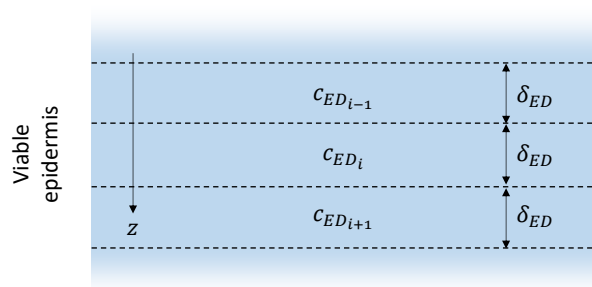
Viable epidermis

$$c_{ED_{i-1}} \qquad \delta_{ED}$$
$$c_{ED_i} \qquad \delta_{ED}$$
$$z \qquad c_{ED_{i+1}} \qquad \delta_{ED}$$

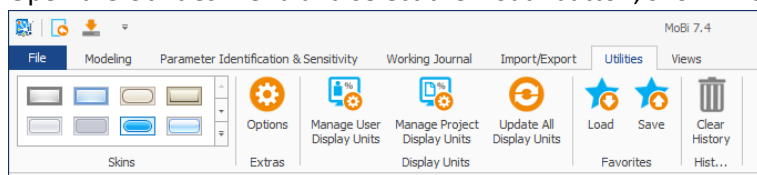*Figure 6: Three sub-sub-layers of the viable epidermis.*

4 Step-by-step setup and simulation of example experiment

The following step-by-step implementation of a testosterone small dose experiment will demonstrate how the model in **skin_permeation_model.mbp3** is used.

4.1 Input of experiment parameters

In this first step, the user enters the parameters of the experiment. These parameters specify the properties of the permeant, the mode of application, the properties of the skin and the parameters of the metabolic reactions consuming the permeant in the viable epidermis and dermis.

1. Open the MoBi model file, **skin_permeation_model.mbp3**.
2. Open the Utilities menu and select the 'Load' button, shown here:

   File | Modeling | Parameter Identification & Sensitivity | Working Journal | Import/Export | Utilities | Views

   MoBi 7.4

   Skins | Options | Manage User Display Units | Manage Project Display Units | Update All Display Units | Load | Save | Clear History
   Extras | Display Units | Favorites | Hist…

3. Select and open the **skin_favorites.xml** file.
4. Expand the 'Spatial Structures' building block in the 'Building Blocks' menu.
5. Double click **skin_spatial_structure** to open its spatial structure window.
6. Under the 'Parameters' tab, select the 'Tree' tab.
7. Click on the 'Favorites' menu item in the 'Tree' tab. This will open a menu of input parameters to be entered, as shown in Figure 9. Example inputs to this menu for a variety of experiments are given in Table 3-Table 7. For the present testosterone small dose experiment, enter the parameters in Table 6 below into their corresponding fields in the 'Favorites' menu.
8. Next, the parameters entered in the 'Favorites' menu will be saved for later use in simulations. To do this, right click on the 'Parameter Start Values' building block in the 'Building Blocks' menu and select 'Create New Parameter Start Values'. Then give these parameters a descriptive name, such as **params_in_vivo_testosterone_small_dose**, and click 'Ok'.

Under 'Molecules' building block menu, the **skin_molecules** building block contains the list of compounds that are included in the simulation. In the example shown in Figure 7, the compound that will be simulated is named 'permeant'. The compound can be given a more descriptive name by right-clicking on 'permeant' and choosing the 'Rename' menu item. However it is important to subsequently also rename the compound's dependent objects when prompted to do so after the new name is input, as in Figure 8.
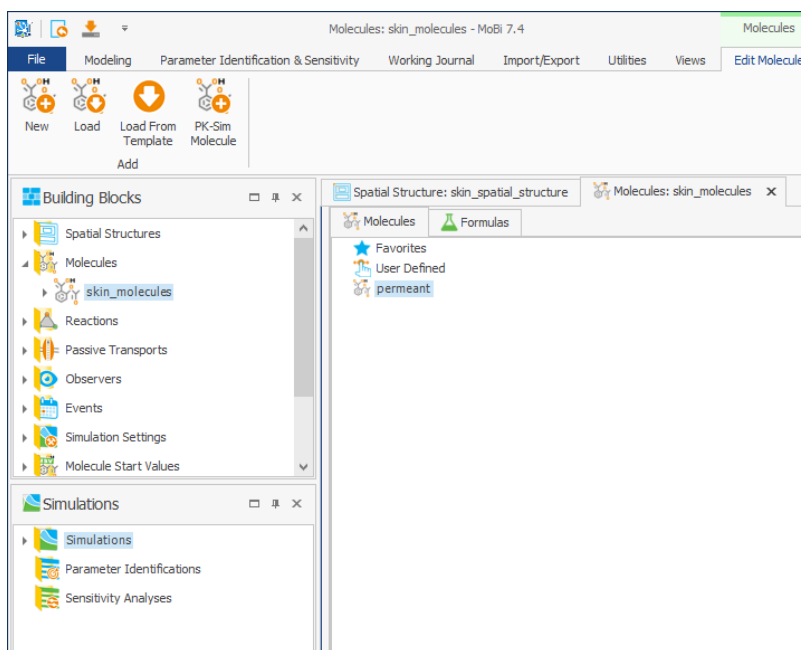
*Figure 7: The compound to be simulated, named 'permeant', is listed in the **skin_molecules** building block.*
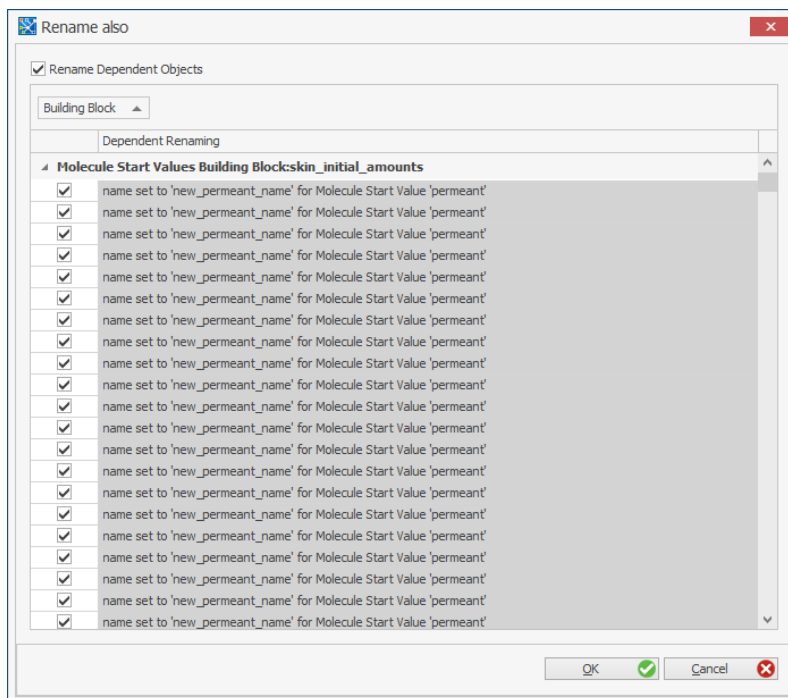

Figure 8: Renaming the objects dependent on the compound, when changing the compound name from 'permeant' to 'new_permeant_name'.

Under the 'Molecule Start Values' building block menu, the **skin_initial_amounts** building block carries formulas needed to compute the initial values of the permeant in the compartments of the MoBi model based on the application scenario and dose size, as per the model in (Dancik et al. 2013). These settings should not be changed for simulation of the model in (Dancik et al. 2013).

4.2   Specification of simulation settings

In this step, the user specifies the length of time for which the experiment will be simulated as well as the accuracy of the simulation.

1. Right click the 'Simulation Settings' building block in the 'Building Blocks' menu and select 'Create Simulation Settings'.
2. Give these simulation settings a descriptive name, such as **settings_testosterone_small_dose**, and click 'Ok'.
3. Enter a 'Start Time' and an 'End Time' for the experiment as well as a 'Resolution' specifying how many simulation time points are needed per unit time.
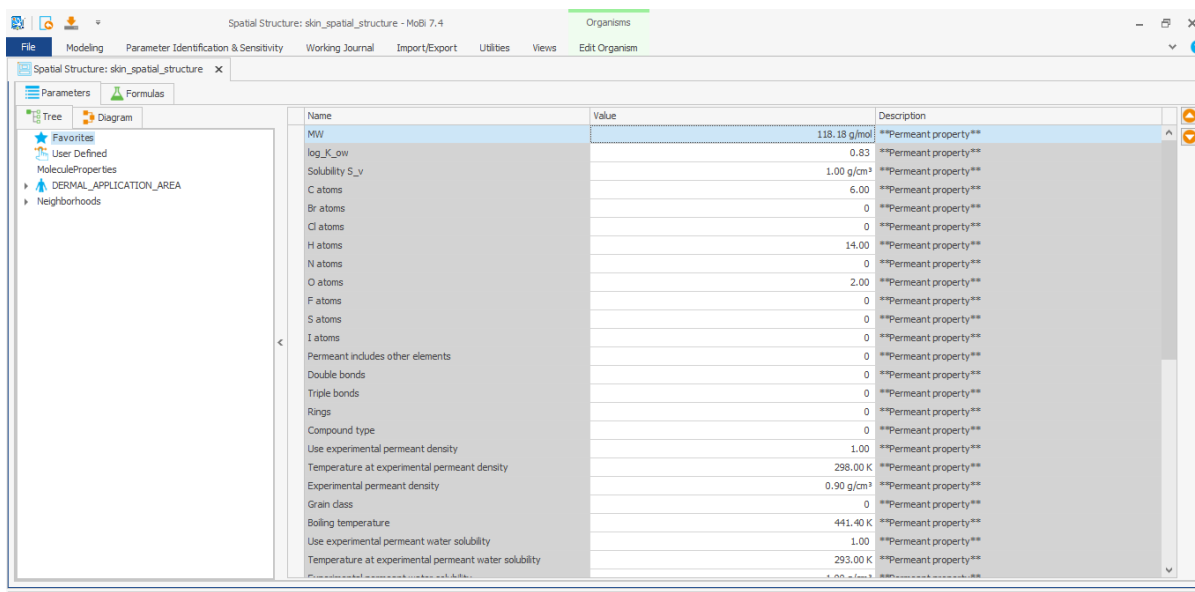

Figure 9: The Favorites menu, in which the user may input the parameters of the model.

4.3   Simulation of the model

Here, the user enters the simulation settings for the desired experiment by selected the appropriate building blocks. A new simulation is created as follows:

1. Right click 'Simulations' in the 'Simulations' window and select 'Create Simulation'. This launches the 'Simulation Creation Wizard'.
2. Give the simulation a name, such as **skin_simulation.**
3. The 'Simulation Settings', 'Molecular Start Values' and 'Parameter Start Values' for the experiment are chosen, as shown in Figure 10.

4. Click on 'Next' three times, followed by 'Ok'. This will launch a window entitled 'Simulation: skin_simulation'.

4.4   Visualization of the simulation results

In order to compare the MoBi simulation results with experimental results in (Dancik et al. 2013), the Observer building block includes observers to generate the simulated estimates of the cumulative amount Q of permeant cleared from the dermis into the bloodstream per square centimeter during the experiment, and the rate J of that clearance.   The maximum values of these estimates that are achieved during the course of the simulated experiments are denoted Q_{abs} and J_{max} in (Dancik et al. 2013), respectively.   With the window entitled 'Simulation: skin_simulation' open, these quantities can be visualized for the present experiment as follows:

1. Select 'Define Settings and Run' from the main toolbar to launch the 'Simulation Settings' menu (Figure 11).
2. Scroll down the list of observable quantities in the top menu of the 'Simulation Settings' menu to the menu items named Q and J in the 'Name' column.
3. Select the checkboxes corresponding to 'Q' and 'J' under the 'Selected' column and click 'Ok'. As shown in Figure 12, this will plot the cumulative amount per 1cm^2 (*Q)* and the flux per 1cm^2 (*J)* over the time course of the experiment, which had been specified in the **settings_testosterone_small_dose** building block.
4. The chart editor can be used to configure the plot settings, including the plot units and appearance. For example, the chart editor was used in Figure 12 to plot Q and J on a linear scale, instead of the default log scale.

Figure 10: Simulation setup for small testosterone dose.
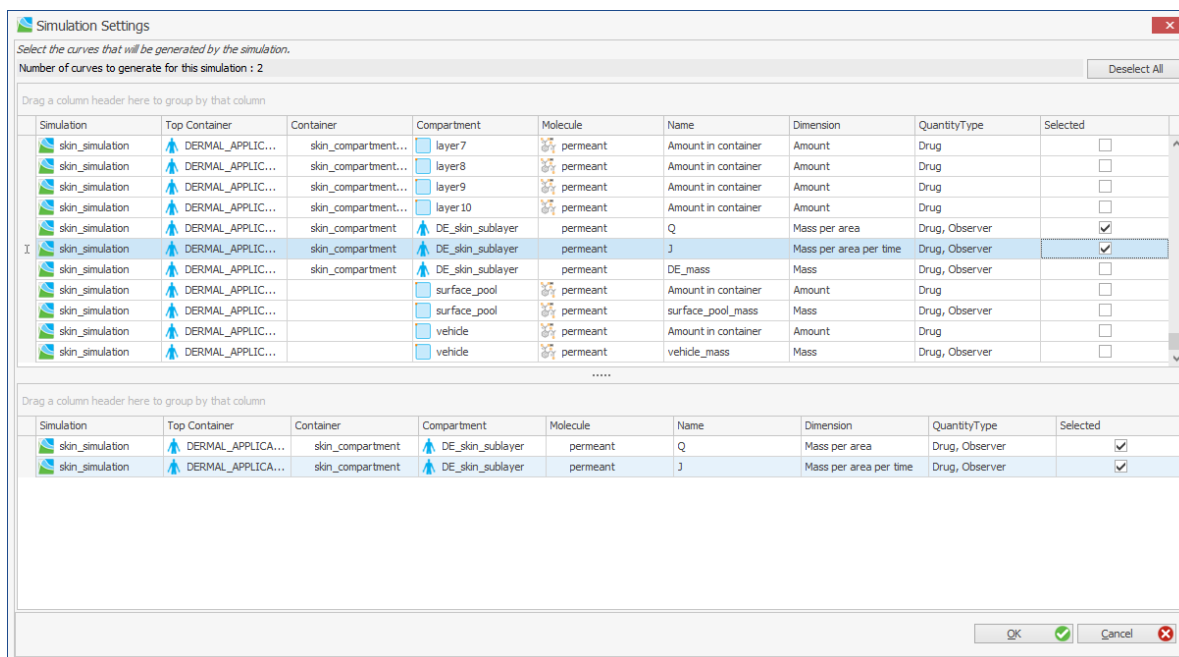
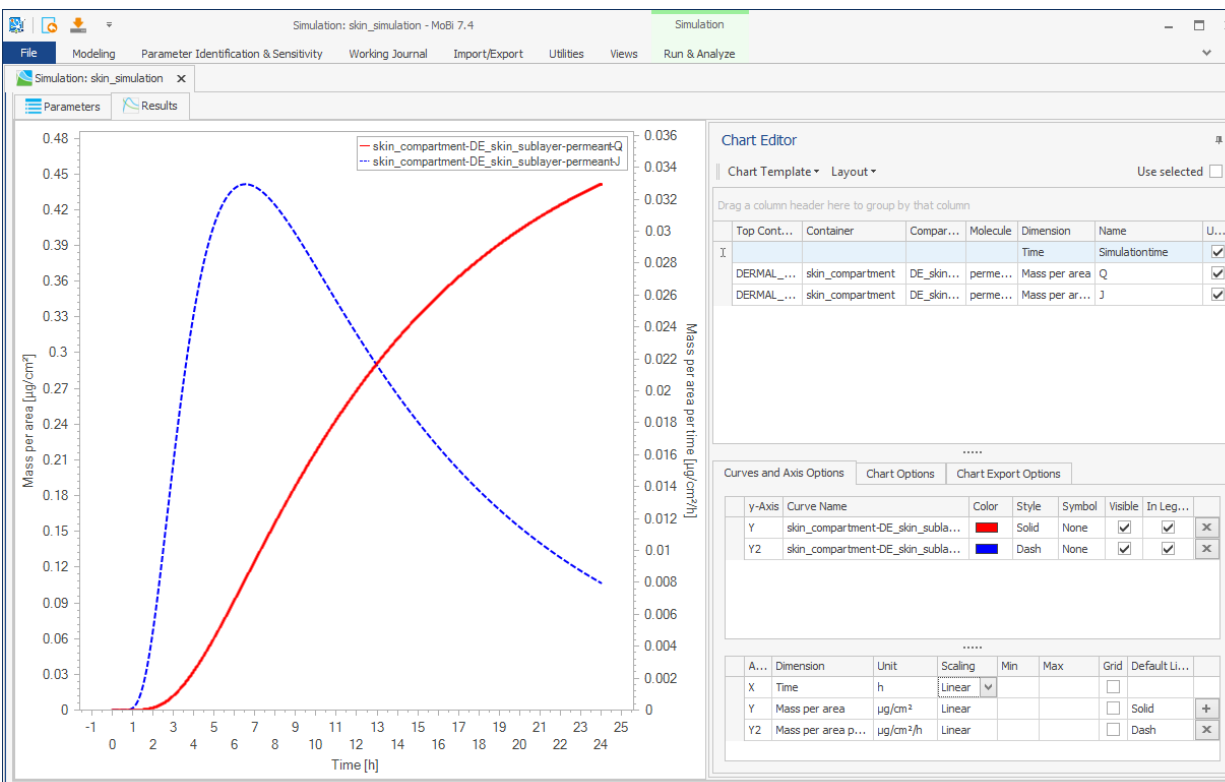*Figure 11: Simulation Settings menu, where the quantities to be plotted are selected.*

Figure 12: Plot of simulation results.

4.5   MoBi model assessment

To assess the model, the MoBi model's estimates of Q_{abs} and J_{max} (defined in (Dancik et al. 2013)) will be compared to their experimentally reported values in (Dancik et al. 2013), to estimates from (Fedorowicz et al. 2011) and to values estimated by Pipeline Pilot.

Permeant and dose type	Maximum cumulative dermis to bloodstream clearance amount Q_{abs} (μg)			
	Experimental	MoBi result	CDC Finite Dose Calculator	Pipeline pilot
DPGME inf. aqueous dose	257	313	274	569
DPGME large dose	609	238	265	571
Testosterone small dose	0.241	0.44	0.45	0.45
Fentanyl inf. aqueous dose	2.00	24	23.8	23.8
2-Butoxyethanol large dose	24211	33563	35012	35072

Permeant and dose type	Maximum rate of dermis to bloodstream clearance amount J_{max} (μg/hour)			
	Experimental	MoBi result	CDC Finite Dose Calculator	Pipeline pilot
DPGME large dose	106	79	82	N/A
Testosterone small dose	0.042	0.033	0.037	N/A
2-Butoxyethanol large dose	1009	1448	1494	N/A

Permeant and dose type	Effective skin permability $k_p \times 10^4$ (cm/h)			
	Experimental	MoBi result	CDC Finite Dose Calculator	Potts-Guy
DPGME inf. aqueous dose	0.8	1.19	1.22	1.66
DPGME large dose		1.19	1.22	1.57
Testosterone small dose		26.5	27.1	71.4
Fentanyl inf. aqueous dose	14.0	163	182	127
2-Butoxyethanol large dose		16.9	16.9	13.3

5   Connecting the dermal model to a whole body PK-Sim model

The following steps outline how the whole-body pharmacokinetics of the dermally applied compound can be simulated by appending the skin permeation model to a whole-body model generated in PK-Sim.

5.1   Step 1: Build and save a MoBi simulation of dermal absorption

Create a simulation by opening **skin_permeation_model.mbp3** and following steps 4.1-4.3 above. The simulation created for this example is named **skin_simulation**, but, since the simulation carries information about the compound, the applied dose and experimental conditions, as specified in the 'Favorites' menu, it is good practice to give the simulation a descriptive name, such as **Testosterone_0p53ug**, for the case of the testosterone experiment with a dose of 0.53µg/cm^2, given in Table 6.

Next, save the simulation in PKML format by right-clicking on the simulation name and selecting 'Save Simulation to MoBi pkml Format', as shown in Figure 13. The default file name for simulation **skin_simulation** is **skin_simulation.pkml**.   Similarly, the default name for the simulation **Testosterone_0p53mg** would be **Testosterone_0p53mg.pkml**. This PKML file can now be reused whenever it is desired to simulate the experiment in Table 6. To conclude this step, close **skin_permeation_model.mbp3**.
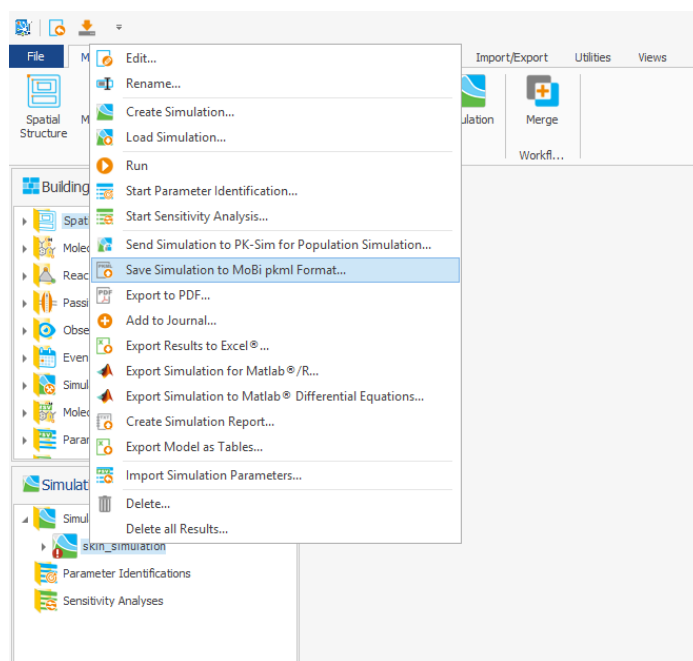
Figure 13: Saving the skin permeation simulation **skin_simulation**.

5.2   Step 2: Build and save a whole-body simulation in PK-Sim

A whole-body simulation is next built using PKSim. Here, it is important to give the compound the same name as that given to the molecule simulated in **skin_simulation**. In our illustrative example, the molecule was named 'permeant', as shown in Figure 7, and this name is used for the compound created in PK-Sim, as shown in Figure 14.

Some of the molecule parameters used in **skin_simulation** will need to be re-entered when creating the PKSim compound. These parameters include the molecular weight, lipophilicity and water solubility. The fraction of the compound molecules unbound to albumin can also be input to the PK-Sim model. This quantity is evaluated by MoBi upon creation of the skin permeation model, **skin_simulation**. Its value can be obtained as shown in Figure 15, by loading the file **skin_simulation.pkml** in MoBi, double-clicking on the simulation name (**skin_simulation**) then double-clicking **skin_compartment**, selecting the 'Parameters' tab and looking up the value of the parameter **FractionUnboundToAlbumin**, which, in this case, is 0.06.

Figure 14: Creating a Compound building block in PK-Sim for later merging with the MoBi skin permeation model.

Once the PK-Sim simulation is created, it is given a descriptive name (in our illustrative example, it is named **whole_body_pksim_simulation**), the simulation is saved in PKML format by right clicking on the simulation name and selecting 'Save Simulation to MoBi pkml Format', as shown in Figure 16. Following the simulation's name, the default file name is **whole_body_pksim_simulation.pkml**.
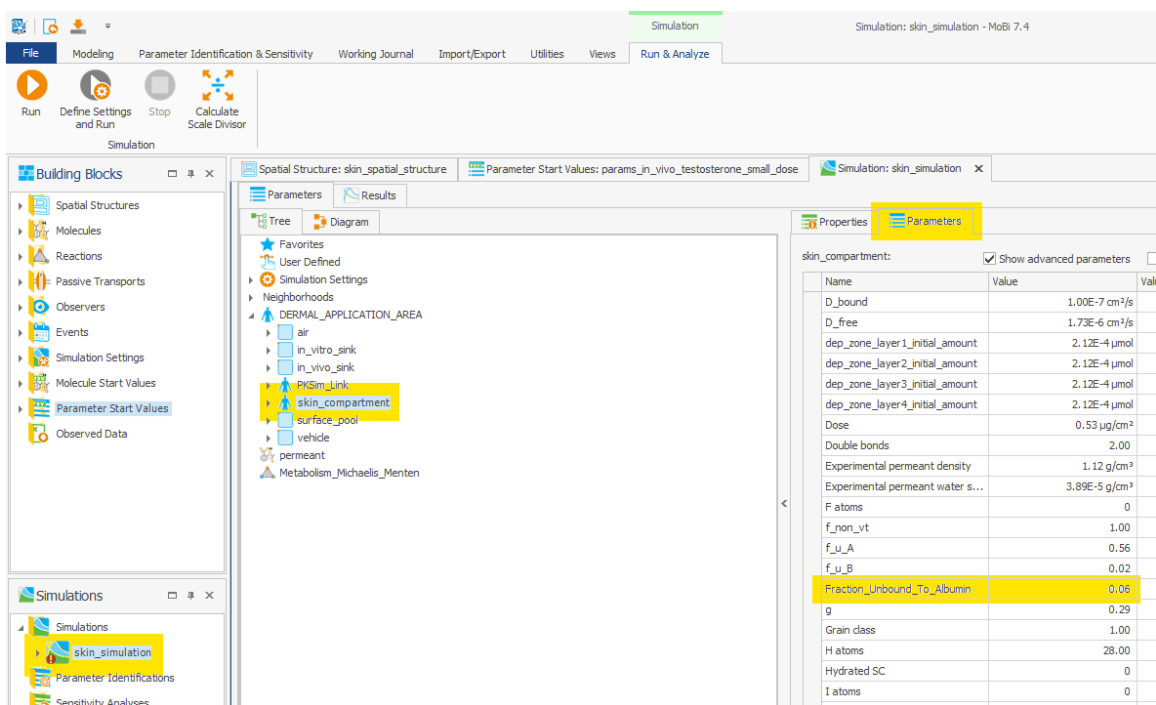
Figure 15: Obtaining the compound's fraction unbound to albumin from the MoBi skin permeation model for input into the PK-Sim whole body model.
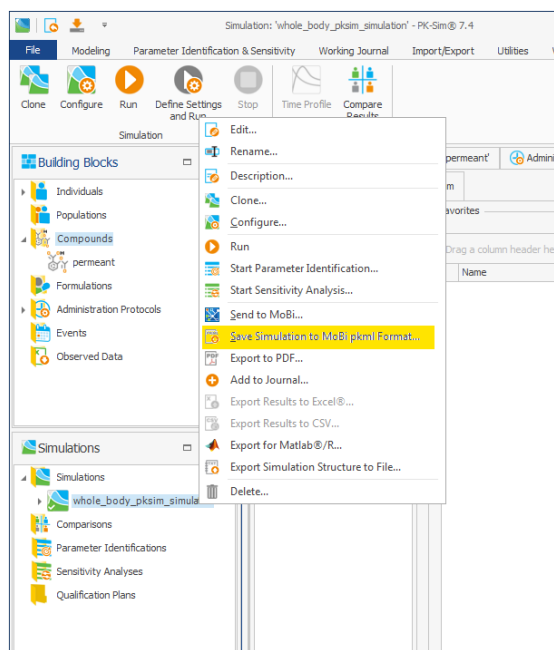

Figure 16: Saving the whole body PK-Sim simulation.

5.3 Step 3: Loading the whole-body and skin models into MoBi

1. In the MoBi 'File' menu, select 'Open Simulation' and select the whole body simulation file **whole_body_pksim_simulation.pkml** generated in PK-Sim in the preceding step. This will load the building blocks of this model into MoBi.

2. Next, double click on **whole_body_pksim_simulation** in the Spatial Structures building block and select the 'Diagram' tab to reveal the whole-body model structure graphically.

3. Next, right-click on the white space adjacent to the model and select 'Load Top Container', as shown in Figure 17. Select the MoBi pkml file **skin_spatial_structure.pkml** that is included in this package, and elect to load the **DERMAL_APPLICATION_AREA** container, as shown in Figure 18. This will load the spatial structure of the skin permeation model, entitled **DERMAL_APPLICATION_AREA** in the white space next to the whole-body model, as shown in Figure 20.

4. Right-click on the **DERMAL_APPLICATION_AREA** spatial structure that was just loaded. Scroll down and hover over the Layout menu item, and select 'Apply Named Template to Selection'. Select the file **skin_template.mbdt**. This file will ameliorate the graphical layout of the new **DERMAL_APPLICATION_AREA** container.

5. As in section 4.1, from the Utilities menu, select 'Load' and then the file **skin_favorites.xml** to load the skin model's 'Favorites' menu. This will allow the user to modify the parameters of the skin compartment from the 'Favorites' menu in the **whole_body_pksim_simulation** building block.
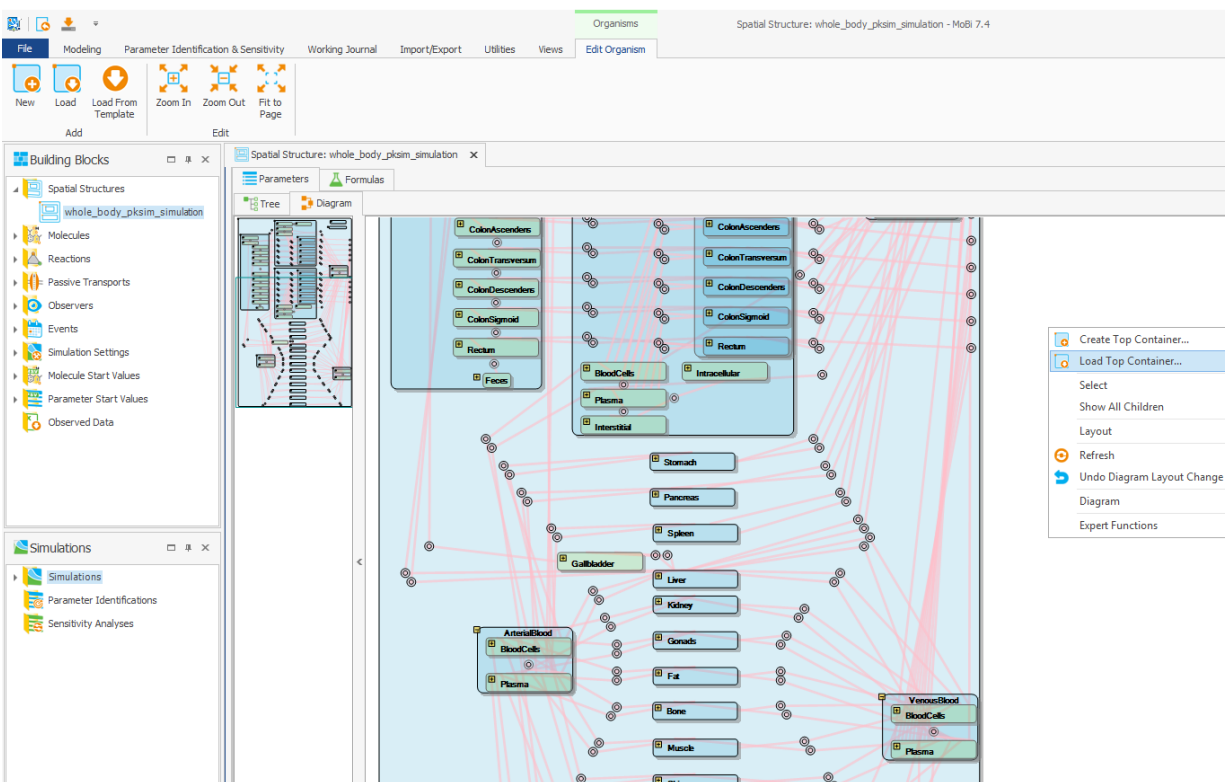
Figure 17: Loading the skin permeation spatial structure in MoBi alongside the whole-body spatial structure previously generated in PK-Sim.
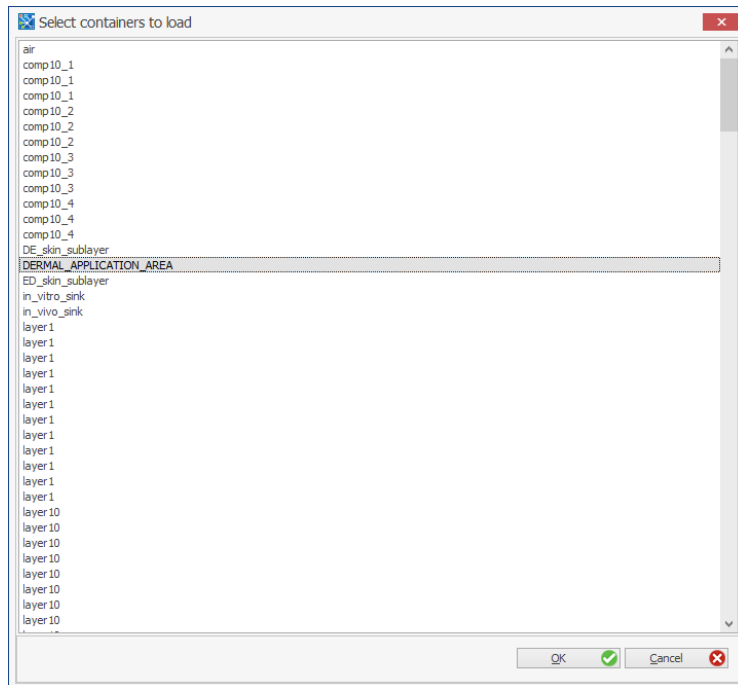
Figure 18: Loading the DERMAL_APPLICATION_AREA container.
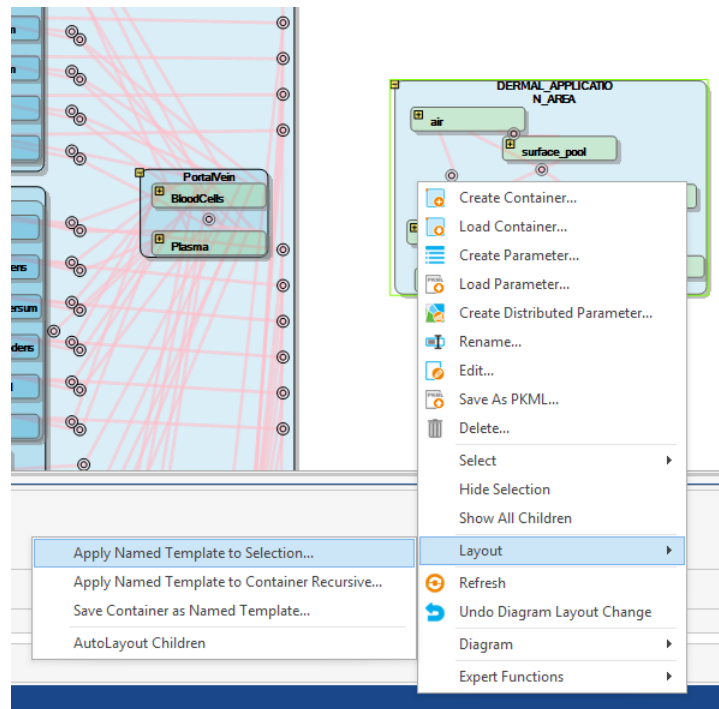
Figure 19: Updating the DERMAL_APPLICATION_AREA layout.

5.4   Step 4: Connect the skin permeation model to the whole body model

Create a neighborhood between the **PKSim_Link** subcompartment of the **DERMAL_APPLICATION_AREA** compartment and the **Plasma** compartment of the **VenousBlood** compartment in the whole body model, giving it a descriptive name, such as **skin_whole_body_neighborhood**. The neighborhood is created by dragging the hand pointer from **PKSim_Link** to the **Plasma** subcompartment of **VenousBlood**. Figure 20 illustrates the end result of this step.
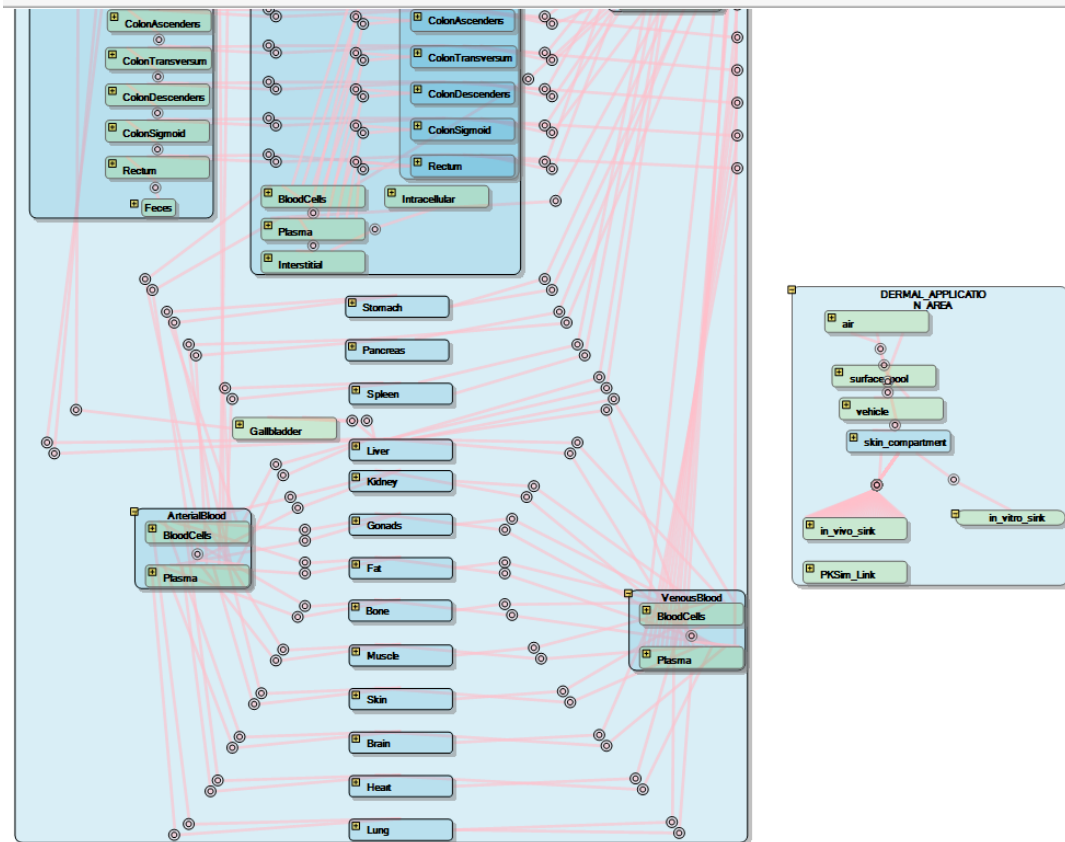
Figure 20: Loading the skin permeation model alongside the whole-body model generated in PK-Sim.
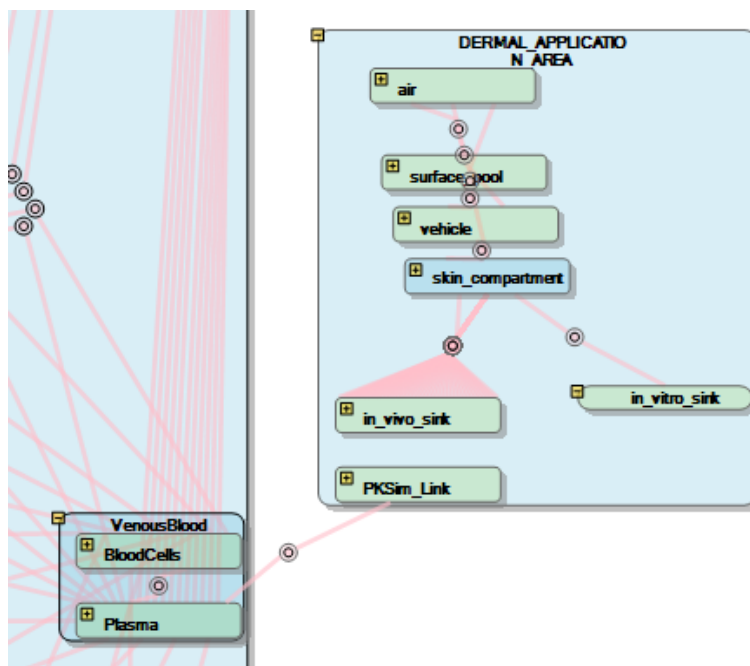
Figure 21: Creating a neighborhood to connect the skin permeation model with the whole-body model.

5.5   Step 5: Load the remaining skin permeation building blocks

So far, all that have been loaded into MoBi are the whole body model and the spatial structure of the skin permeation model. Before the integrated whole-body and skin permeation model can be simulated, the building blocks from the skin permeation model, which were previously saved in Step 1 in **skin_simulation.pkml**, need to be loaded. To do so select the Modeling menu in MoBi, and click the 'Merge' button, shown on the right of this image:
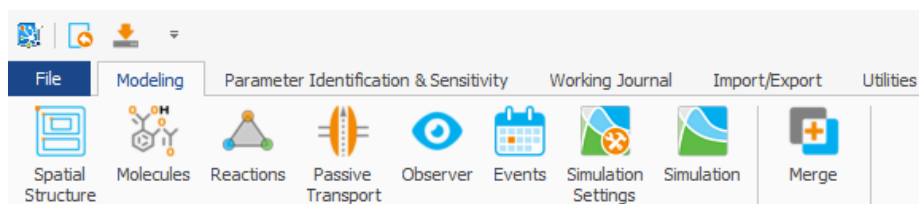
Load the file **skin_simulation.pkml** into 'Simulation path'. This gives the user the option to merge building blocks from **skin_simulation** with the building blocks in **whole_body_pksim_simulation**. All building blocks except the **Molecules** building block **skin_molecules** and the **skin_events** building block named **Events** should be merged with their corresponding blocks in **whole_body_pksim_simulation**.
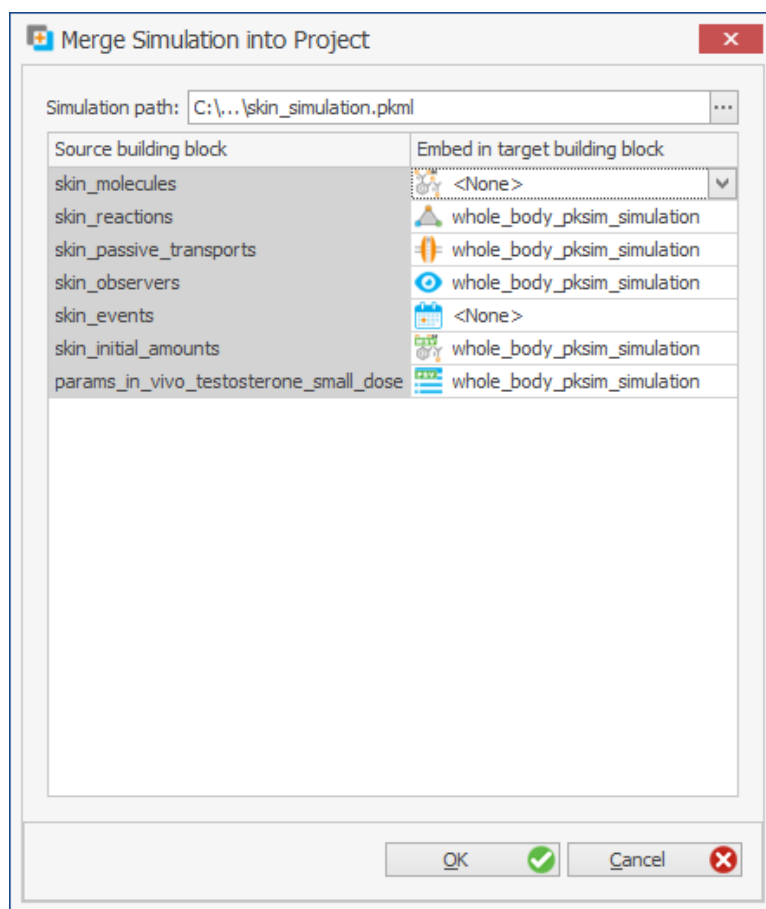
*Figure 22: Merging of the building blocks from **skin_simulation** with those from **whole_body_pksim_simulation**.*

5.6   Step 6: Simulate the integrated model

The skin permeation and whole body model is now integrated and can be simulated. A simulation may be created as described previously, by right clicking on 'Simulations' and selecting 'Create Simulation'. The Simulation Creation Wizard menu will prompt the user to select the building blocks. The user should select the building blocks which were merged together in the previous step, as shown in Figure 23.
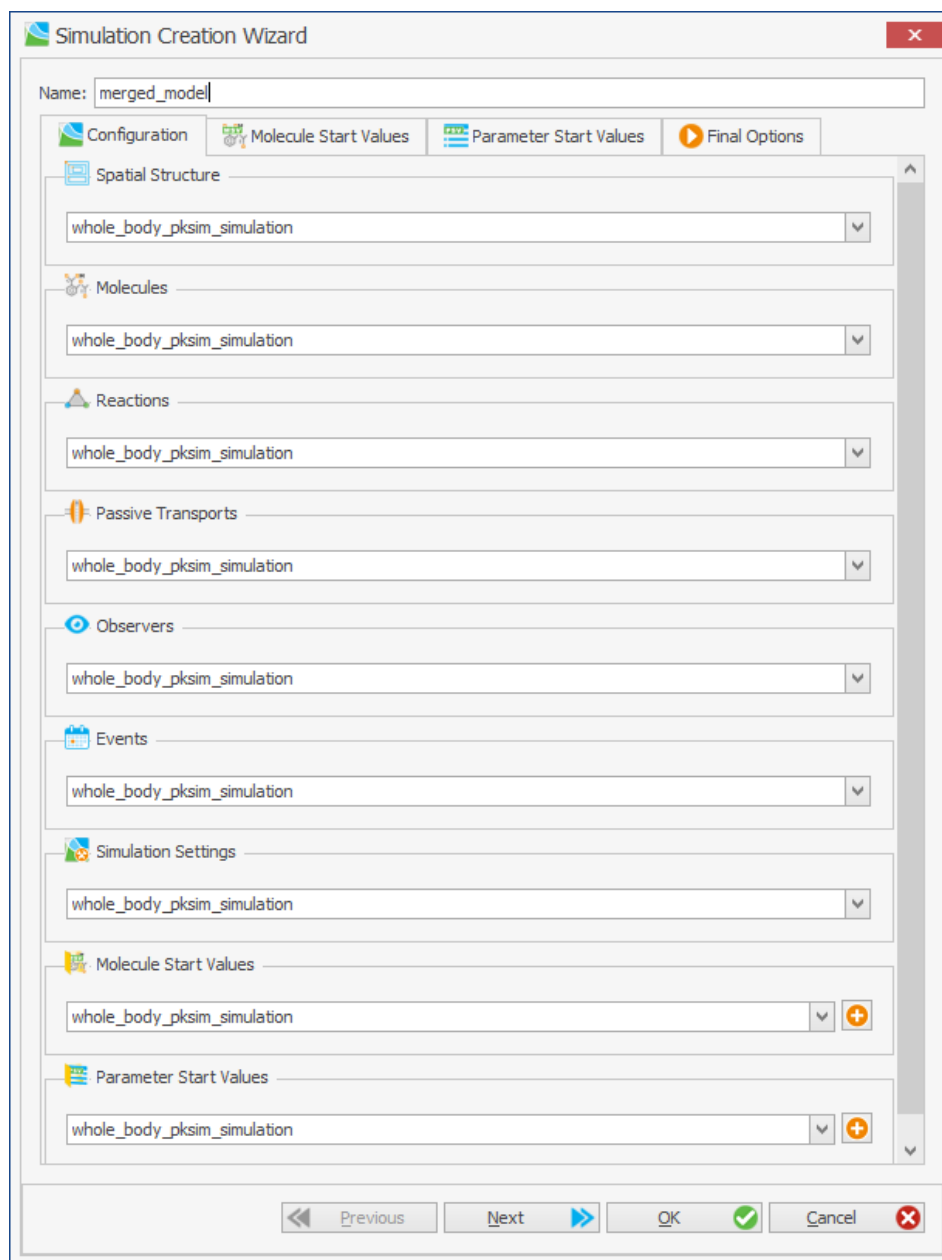
Figure 23: Creating a simulation of the merged model.

Once the simulation is complete, the user may plot graphs of quantities in any desired compartment of the model. The example in Figure 24 shows the simulated amount of permeant present in the stratum corneum (SC), epidermis (ED), dermis (DE) and in liver plasma.
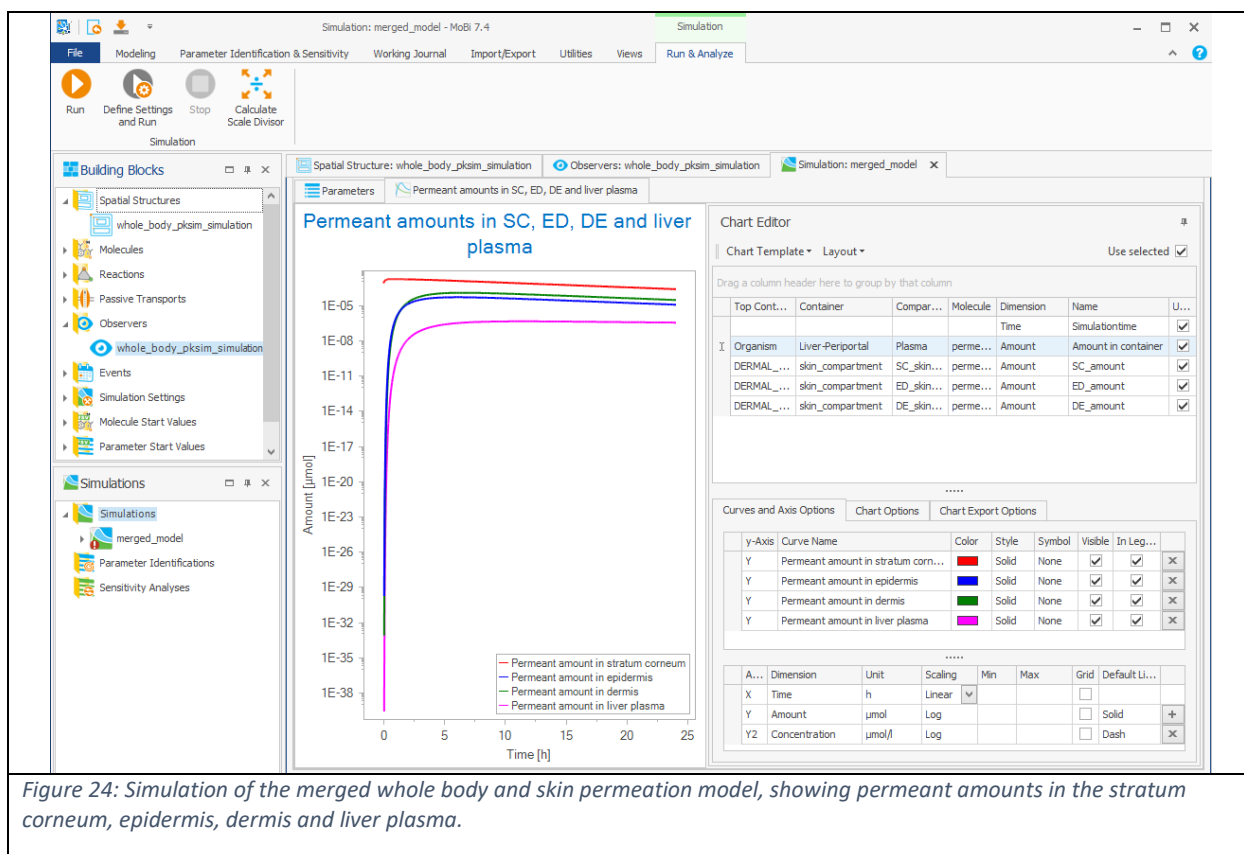
Figure 24: Simulation of the merged whole body and skin permeation model, showing permeant amounts in the stratum corneum, epidermis, dermis and liver plasma.

6 Input parameters for experiments

6.1 2-butoxyethanol– large dose, 24 hours

Model parameters

Property	Value	Units/format
Permeant properties		
Molecular weight MW	118.18	g.mol^{-1}
$\log K_{o/w}$	0.83	Dimensionless
Solubility S_v	1	g.cm^{-3}
C atoms	6	Non-negative integer
Br atoms	0	Non-negative integer
Cl atoms	0	Non-negative integer
H atoms	14	Non-negative integer
N atoms	0	Non-negative integer
O atoms	2	Non-negative integer
F atoms	0	Non-negative integer
S atoms	0	Non-negative integer
I atoms	0	Non-negative integer
Permeant includes other elements	0	0 - No, 1 - Yes
Number of double bonds	0	Non-negative integer
Number of triple bonds	0	Non-negative integer
Number of rings	0	Non-negative integer
Compound type	0	0 - Neutral compound, 1 - Basic compound, 2 - Acid with pharmacophore, 3 - Acid without pharmacophore, 4 - Zwitterion
Use experimental permeant density	1	0 - No, 1 - Yes
Temperature at experimental permeant density	25	Celsius
Experimental permeant density	0.899	g.cm^{-3}
Grain class	0	0 - Alcohol, 1 – Hydrocarbon, 2 - Other organic compound
Boiling temperature	168.4	Celsius
Use experimental permeant water solubility	1	0 - No, 1 - Yes
Temperature at experimental permeant water solubility	20	Celsius
Experimental permeant water solubility	1	g.cm^{-3}
Melting temperature	-74.8	Celsius
Use strongest acid pK$_a$	0	0 - No, 1 - Yes
Strongest acid pK$_a$	0	Dimensionless
Use strongest base pK$_a$	0	0 - No, 1 - Yes
Strongest base pK$_a$	0	Dimensionless
Vapor pressure	0	mmHg
Application properties		
Dose	281250	µg.cm^{-2}
Area of application	1	cm^2
Wind velocity	16.8	cm.s^{-1}
Occluded vehicle	1	0 - Not occluded, 1 - Occluded
Vehicle type	0	0 - No vehicle, 1 – Water, 2 – Ethanol, 3 – Acetone, 4 - Other
Volatile vehicle	1	0 - Vehicle not volatile, 1 - Vehicle is volatile
Vehicle pH	7.4	Dimensionless
Vehicle volume	0	cm^3
Skin properties		
Skin temperature	30	Celsius
Hydrated SC	1	0=Partially hydrated SC, 1 = Hydrated SC
Skin thickness	0.5	mm
In vivo	1	0 - in vitro, 1 - in vivo
Metabolism properties		
V_{max}	0	s^{-1}
K_M	1	µmol.L^{-1}

Table 3: Input parameters for MoBi 2-butoxyethanol large dose, 24 hour simulation.

6.2 DPGME – infinite aqueous dose, 8 hours

Model parameters

Property	Value	Units/format
Permeant properties		
Molecular weight MW	148.20	g.mol^{-1}
$\log K_{o/w}$	-0.22	Dimensionless
Solubility S_v	0.96	g.cm^{-3}
C atoms	7	Non-negative integer
Br atoms	0	Non-negative integer
Cl atoms	0	Non-negative integer
H atoms	16	Non-negative integer
N atoms	0	Non-negative integer
O atoms	3	Non-negative integer
F atoms	0	Non-negative integer
S atoms	0	Non-negative integer
I atoms	0	Non-negative integer
Permeant includes other elements	0	0 - No, 1 - Yes
Number of double bonds	0	Non-negative integer
Number of triple bonds	0	Non-negative integer
Number of rings	0	Non-negative integer
Compound type	0	0 - Neutral compound, 1 - Basic compound, 2 - Acid with pharmacophore, 3 - Acid without pharmacophore, 4 - Zwitterion
Use experimental permeant density	1	0 - No, 1 - Yes
Temperature at experimental permeant density	25	Celsius
Experimental permeant density	0.96	g.cm^{-3}
Grain class	0	0 - Alcohol, 1 – Hydrocarbon, 2 - Other organic compound
Boiling temperature	188	Celsius
Use experimental permeant water solubility	1	0 - No, 1 - Yes
Temperature at experimental permeant water solubility	25	Celsius
Experimental permeant water solubility	0.93	g.cm^{-3}
Melting temperature	-80	Celsius
Use strongest acid pK$_a$	0	0 - No, 1 - Yes
Strongest acid pK$_a$	0	Dimensionless
Use strongest base pK$_a$	0	0 - No, 1 - Yes
Strongest base pK$_a$	0	Dimensionless
Vapor pressure	0.14	mmHg
Application properties		
Dose	9.3×10^4	µg.cm^{-2}
Area of application	1	cm^2
Wind velocity	16.8	cm.s^{-1}
Occluded vehicle	1	0 - Not occluded, 1 - Occluded
Vehicle type	1	0 - No vehicle, 1 – Water, 2 – Ethanol, 3 – Acetone, 4 - Other
Volatile vehicle	1	0 - Vehicle not volatile, 1 - Vehicle is volatile
Vehicle pH	7.4	Dimensionless
Vehicle volume	0.2	cm^3
Skin properties		
Skin temperature	30	Celsius
Hydrated SC	1	0=Partially hydrated SC, 1 = Hydrated SC
Skin thickness	1	mm
In vivo	1	0 - in vitro, 1 - in vivo
Metabolism properties		
V_{max}	0	s^{-1}
K_M	1	µmol.L^{-1}

Table 4: Input parameters for DPGME infinite aqueous dose 8 hour simulation.

6.3 DPGME – large dose, 8 hours

Model Parameters

Property	Value	Units/format
Permeant properties		
Molecular weight MW	148.20	g.mol^{-1}
$\log K_{o/w}$	0.95	Dimensionless
Solubility S_v	-0.22	g.cm^{-3}
C atoms	7	Non-negative integer
Br atoms	0	Non-negative integer
Cl atoms	0	Non-negative integer
H atoms	16	Non-negative integer
N atoms	0	Non-negative integer
O atoms	3	Non-negative integer
F atoms	0	Non-negative integer
S atoms	0	Non-negative integer
I atoms	0	Non-negative integer
Permeant includes other elements	0	0 - No, 1 - Yes
Number of double bonds	0	Non-negative integer
Number of triple bonds	0	Non-negative integer
Number of rings	0	Non-negative integer
Compound type	0	0 - Neutral compound, 1 - Basic compound, 2 - Acid with pharmacophore, 3 - Acid without pharmacophore, 4 - Zwitterion
Use experimental permeant density	1	0 - No, 1 - Yes
Temperature at experimental permeant density	30	Celsius
Experimental permeant density	1.12	g.cm^{-3}
Grain class	1	0 - Alcohol, 1 – Hydrocarbon, 2 - Other organic compound
Boiling temperature	188	Celsius
Use experimental permeant water solubility	1	0 - No, 1 - Yes
Temperature at experimental permeant water solubility	30	Celsius
Experimental permeant water solubility	3.89×10^{-5}	g.cm^{-3}
Melting temperature	-80	Celsius
Use strongest acid pK$_a$	0	0 - No, 1 - Yes
Strongest acid pK$_a$	0	Dimensionless
Use strongest base pK$_a$	0	0 - No, 1 - Yes
Strongest base pK$_a$	0	Dimensionless
Vapor pressure	5.75×10^{-8}	mmHg

Property	Value	Units/format
Application properties		
Dose	1.9×10^5	µg.cm^{-2}
Area of application	1	cm^2
Wind velocity	16.8	cm.s^{-1}
Occluded vehicle	1	0 - Not occluded, 1 - Occluded
Vehicle type	0	0 - No vehicle, 1 – Water, 2 – Ethanol, 3 – Acetone, 4 - Other
Volatile vehicle	1	0 - Vehicle not volatile, 1 - Vehicle is volatile
Vehicle pH	7.4	Dimensionless
Vehicle volume	0.2	cm^3

Property	Value	Units/format
Skin properties		
Skin temperature	30	Celsius
Hydrated SC	1	0=Partially hydrated SC, 1 = Hydrated SC
Skin thickness	1	mm
In vivo	1	0 - in vitro, 1 - in vivo

Property	Value	Units/format
Metabolism properties		
V_{max}	0	s^{-1}
K_M	1	µmol.L^{-1}

Table 5: Input parameters for DPGME large dose 8 hour simulation.

6.4 Testosterone – small dose, 24 hours

Model parameters

Property	Value	Units/format
Permeant properties		
Molecular weight MW	288.43	$g.mol^{-1}$
$\log K_{o/w}$	3.32	Dimensionless
Solubility S_v	3.89×10^{-5}	$g.cm^{-3}$
C atoms	19	Non-negative integer
Br atoms	0	Non-negative integer
Cl atoms	0	Non-negative integer
H atoms	28	Non-negative integer
N atoms	0	Non-negative integer
O atoms	2	Non-negative integer
F atoms	0	Non-negative integer
S atoms	0	Non-negative integer
I atoms	0	Non-negative integer
Permeant includes other elements	0	0 - No, 1 - Yes
Number of double bonds	2	Non-negative integer
Number of triple bonds	0	Non-negative integer
Number of rings	4	Non-negative integer
Compound type	0	0 - Neutral compound, 1 - Basic compound, 2 - Acid with pharmacophore, 3 - Acid without pharmacophore, 4 - Zwitterion
Use experimental permeant density	1	0 - No, 1 - Yes
Temperature at experimental permeant density	30	Celsius
Experimental permeant density	1.12	$g.cm^{-3}$
Grain class	1	0 - Alcohol, 1 – Hydrocarbon, 2 - Other organic compound
Boiling temperature	433	Celsius
Use experimental permeant water solubility	1	0 - No, 1 - Yes
Temperature at experimental permeant water solubility	35	Celsius
Experimental permeant water solubility	3.89×10^{-5}	$g.cm^{-3}$
Melting temperature	155	Celsius
Use strongest acid pK_a	0	0 - No, 1 - Yes
Strongest acid pK_a	0	Dimensionless
Use strongest base pK_a	0	0 - No, 1 - Yes
Strongest base pK_a	0	Dimensionless
Vapor pressure	5.75×10^{-8}	mmHg

Property	Value	Units/format
Application properties		
Dose	0.53	$\mu g.cm^{-2}$
Area of application	1	cm^2
Wind velocity	16.8	$cm.s^{-1}$
Occluded vehicle	0	0 - Not occluded, 1 - Occluded
Vehicle type	1	0 - No vehicle, 1 – Water, 2 – Ethanol, 3 – Acetone, 4 - Other
Volatile vehicle	1	0 - Vehicle not volatile, 1 - Vehicle is volatile
Vehicle pH	7.4	Dimensionless
Vehicle volume	25×10^{-3}	cm^3

Property	Value	Units/format
Skin properties		
Skin temperature	30	Celsius
Hydrated SC	0	0=Partially hydrated SC, 1 = Hydrated SC
Skin thickness	0.5	mm
In vivo	1	0 - in vitro, 1 - in vivo

Property	Value	Units/format
Metabolism properties		
V_{max}	0	s^{-1}
K_M	1	$\mu mol.L^{-1}$

Table 6: Input parameters for testosterone small dose 24 hour simulation.

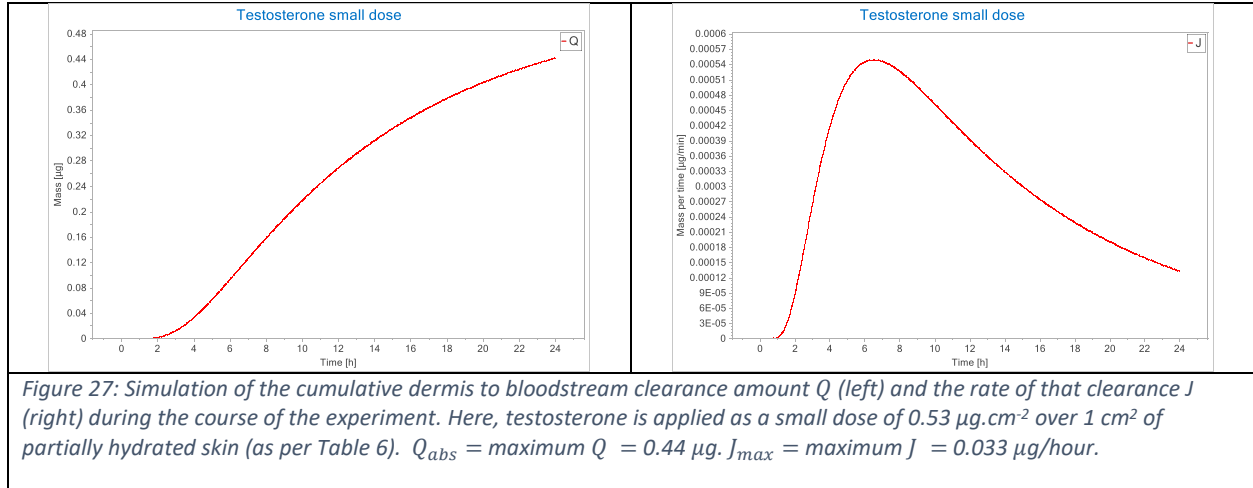## 6.5 Fentanyl – infinite aqueous dose, 72 hours

Model parameters

Property	Value	Units/format
Permeant properties		
Molecular weight MW	336.47	$g.mol^{-1}$
$\log K_{o/w}$	4.05	Dimensionless
Solubility S_v		$g.cm^{-3}$
C atoms	22	Non-negative integer
Br atoms	0	Non-negative integer
Cl atoms	0	Non-negative integer
H atoms	28	Non-negative integer
N atoms	2	Non-negative integer
O atoms	1	Non-negative integer
F atoms	0	Non-negative integer
S atoms	0	Non-negative integer
I atoms	0	Non-negative integer
Permeant includes other elements	0	0 - No, 1 - Yes
Number of double bonds	7	Non-negative integer
Number of triple bonds	0	Non-negative integer
Number of rings	3	Non-negative integer
Compound type	0	0 - Neutral compound, 1 - Basic compound, 2 - Acid with pharmacophore, 3 - Acid without pharmacophore, 4 - Zwitterion
Use experimental permeant density	1	0 - No, 1 - Yes
Temperature at experimental permeant density	25	Celsius
Experimental permeant density	1.09	$g.cm^{-3}$
Grain class	2	0 - Alcohol, 1 – Hydrocarbon, 2 - Other organic compound
Boiling temperature	466	Celsius
Use experimental permeant water solubility	1	0 - No, 1 - Yes
Temperature at experimental permeant water solubility	25	Celsius
Experimental permeant water solubility	24	$g.cm^{-3}$
Melting temperature	88	Celsius
Use strongest acid pK$_a$	0	0 - No, 1 - Yes
Strongest acid pK$_a$	0	Dimensionless
Use strongest base pK$_a$	1	0 - No, 1 - Yes
Strongest base pK$_a$	8.9	Dimensionless
Vapor pressure	0	mmHg

Property	Value	Units/format
Application properties		
Dose	24	$\mu g.cm^{-2}$
Area of application	1	cm^2
Wind velocity	16.8	$cm.s^{-1}$
Occluded vehicle	1	0 - Not occluded, 1 - Occluded
Vehicle type	1	0 - No vehicle, 1 – Water, 2 – Ethanol, 3 – Acetone, 4 - Other
Volatile vehicle	0	0 - Vehicle not volatile, 1 - Vehicle is volatile
Vehicle pH	7.4	Dimensionless
Vehicle volume	0.472	cm^3

Property	Value	Units/format
Skin properties		
Skin temperature	30	Celsius
Hydrated SC	1	0=Partially hydrated SC, 1 = Hydrated SC
Skin thickness	1	mm
In vivo	1	0 - in vitro, 1 - in vivo

Property	Value	Units/format
Metabolism properties		
V_{max}	0	s^{-1}
K_M	1	$\mu mol.L^{-1}$

Table 7: Input parameters for fentanyl infinite aqueous dose 72 hour simulation.

7 Simulation results

Figure 25: Simulation of the cumulative dermis to bloodstream clearance amount Q collected during the course of the experiment. Here, DPGME is applied as an infinite aqueous dose of $9.3×10^4$ µg.cm^{-2} over 1 cm^2 of fully hydrated skin (as per Table 4). Here, the maximum value of Q over the time course of the simulated experiment is Q_{abs}=313 µg.

Figure 26: Simulation of the cumulative dermis to bloodstream clearance amount Q (left) and the rate of that clearance J (right) during the course of the experiment. Here, DPGME is applied as a large dose of $1.9×10^5$ µg.cm^{-2} over 1 cm^2 of fully hydrated skin (as per Table 5). Q_{abs} = maximum Q=238 µg. J_{max} = maximum J=79 µg/hour.

Figure 27: Simulation of the cumulative dermis to bloodstream clearance amount Q (left) and the rate of that clearance J (right) during the course of the experiment. Here, testosterone is applied as a small dose of 0.53 µg.cm⁻² over 1 cm² of partially hydrated skin (as per Table 6). Q_{abs} = maximum Q = 0.44 µg. J_{max} = maximum J = 0.033 µg/hour.

8 Appendix

Numerical implementation of boundary conditions in Table 1 and Table 2 will be demonstrated using the SC/ED interface as an example. This region is illustrated in Figure 28. The SC is divided into thin layers of thickness δ_{SC} and concentrations c_{SC_i} ($i = N, N-1, \cdots$). The ED is similarly divided into thin layers of thickness δ_{ED} and concentrations c_{ED_i} ($i = 1,2,\cdots$). The flux of the permeant into the top of the SC region is denoted by u_{in}, and the permeant flux out of the bottom of the ED by u_{out}.
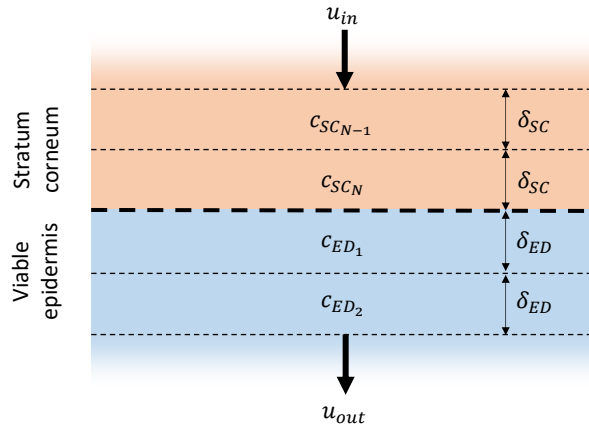

Figure 28: Illustration of numerical approximation of permeant concentrations near the SC/ED boundary. Quantities u_{in} and u_{out} represent the flux of permeant into and out of this region, respectively

Fick's law and mass balance are used to approximate the rate of change of concentration in each layer as:

$$\dot{c}_{SC_{N-1}} = u_{in} - \frac{D_{SC}}{\delta_{SC}}(c_{SC_{N-1}} - c_{SC_N})$$

$$\dot{c}_{SC_N} = \frac{D_{SC}}{\delta_{SC}}(c_{SC_{N-1}} - c_{SC_N}) - \frac{1}{\epsilon}\left(\frac{c_{SC_N}}{K_{SC}} - \frac{c_{ED_1}}{K_{ED}}\right)$$

$$\dot{c}_{ED_1} = \frac{1}{\epsilon}\left(\frac{c_{SC_N}}{K_{SC}} - \frac{c_{ED_1}}{K_{ED}}\right) - \frac{D_{ED}}{\delta_{ED}}(c_{ED_1} - c_{ED_2})$$

$$\dot{c}_{ED_2} = \frac{D_{ED}}{\delta_{ED}}\left(c_{ED_1} - c_{ED_2}\right) - u_{out}$$

The quantity ϵ is small, representing the fact that the two concentrations of the permeant in the layers at the interface of the SC and ED quickly reach an equilibrium dependent on the partition coefficients of the two layers $\frac{c_{SC_N}}{K_{SC}} = \frac{c_{ED_1}}{K_{ED}}$. Letting $c = c_{SC_N} + c_{ED_1}$ gives the system

$$\dot{c}_{SC_{N-1}} = u_{in} - \frac{D_{SC}}{\delta_{SC}}\left(c_{SC_{N-1}} - c_{SC_N}\right)$$

$$\dot{c} = \frac{D_{SC}}{\delta_{SC}}\left(c_{SC_{N-1}} - c_{SC_N}\right) - \frac{D_{ED}}{\delta_{ED}}\left(c_{ED_1} - c_{ED_2}\right)$$

$$\dot{c}_{ED_2} = \frac{D_{ED}}{\delta_{ED}}\left(c_{ED_1} - c_{ED_2}\right) - u_{out}$$

From mass balance, the flux of permeant leaving the SC must equal the flux of permeant entering the ED. Fick's law can be used to approximate this mass balance relation as:

$$\frac{D_{SC}}{\delta_{SC}}\left(c_{SC_{N-1}} - c_{SC_N}\right) = \frac{D_{ED}}{\delta_{ED}}\left(c_{ED_1} - c_{ED_2}\right)$$

This implies that $\dot{c} = 0$. From the above relations, it follows, after some work, that

$$\dot{c}_{SC_{N-1}} = u_{in} - \frac{1}{F}\left(\beta c_{SC_{N-1}} - c_{ED_2}\right)$$

$$\dot{c}_{ED_2} = \frac{1}{F}\left(\beta c_{SC_{N-1}} - c_{ED_2}\right) - u_{out}$$

Where $\beta = \frac{K_{ED}}{K_{SC}}$, $F = F_{SC} + F_{ED}$, $F_{SC} = \frac{\delta_{SC}}{D_{SC}}$ and $F_{ED} = \frac{\delta_{ED}}{\beta D_{ED}}$. By analogy with Ohm's law, F_{SC} and F_{ED} can be viewed as measures of the 'resistance' to the flow ('current') of permeant in the SC and ED, driven by the scaled concentration difference ('potential difference') $\beta c_{SC_{N-1}} - c_{ED_2}$.

9   References

Dancik, Yuri, Matthew A. Miller, Joanna Jaworska, and Gerald B. Kasting. 2013. "Design and Performance of a Spreadsheet-Based Model for Estimating Bioavailability of Chemicals from Dermal Exposure." *Advanced Drug Delivery Reviews*. https://doi.org/10.1016/j.addr.2012.01.006.

Fedorowicz, Adam, Matthew Miller, Gerald Kasting, and H. Frederick Frasch. 2011. "Finite Dose Skin Permeation Calculator." National Institute for Occupational Safety and Health. https://www.cdc.gov/niosh/topics/skin/finiteskinpermcalc.html.

Kasting, Gerald B., and Matthew A. Miller. 2006. "Kinetics of Finite Dose Absorption through Skin 2: Volatile Compounds." *Journal of Pharmaceutical Sciences* 95 (2): 268–80. https://doi.org/10.1002/jps.20497.

Potts, Russell O., and Richard H. Guy. 1992. "Predicting Skin Permeability." *Pharmaceutical Research* 9 (5): 663–69.